

10 World Conference on Neutron Radiography 5-10 October 2014

A New Cold Neutron Imaging Instrument at NIST

D.S. Hussey^{a,1}, C. Brocker^b, J.C. Cook^b, D.L. Jacobson^a, T.R. Gentile^a, W.C. Chen^b, E. Baltic^a, D.V. Baxter^c, J. Daskow^c, and M. Arif^a

^aNeutron Physics Group, NIST, Gaithersburg, MD, 20899 USA

^bNIST Center for Neutron Research, NIST, Gaithersburg, MD, 20899 USA

^cCenter for the Exploration of Energy and Matter, Indiana University, Bloomington, IN, 47408 USA

Abstract

The NIST neutron imaging program will build a new imaging instrument in the NCNR guide hall at the end of the neutron guide NG-6, beginning operation in summer of 2015. The NG-6 guide has a spectrum that is strongly peaked at a neutron wavelength of 0.5 nm, with a fluence rate of $2 \times 10^9 \text{ cm}^{-2} \text{ s}^{-1}$ before a bismuth filter that is cooled by liquid nitrogen. The instrument will be developed in a phased manner and with an emphasis on maintaining a flexible space to conduct experiments and test new instrument concepts. In the initial phase of the instrument, the available space will permit a flight path of about 9 m, and will provide a platform for standard neutron radiography and tomography, wavelength selective imaging with a double crystal monochromator, and phase imaging based on a Talbot-Lau interferometer. The novel feature of the instrument will be the incorporation of Wolter optics to create a neutron microscope. Initially, prototype optics will be used in the microscope configuration to assess optic characteristics and image acquisition techniques. In the final form, the microscope will enable users to acquire images with $\sim 10 \mu\text{m}$ resolution 10-100x faster than current practice, and with a 10x magnifying optic to acquire images with $\sim 1 \mu\text{m}$ spatial resolution with image acquisition time similar to that for current images with $\sim 10 \mu\text{m}$ resolution.

Published by Elsevier B.V. This is an open access article under the CC BY-NC-ND license

(<http://creativecommons.org/licenses/by-nc-nd/4.0/>).

Selection and peer-review under responsibility of Paul Scherrer Institut

Keywords:

microscope; Talbot-Lau interferometer; cold neutron

neutron phase imaging; grating interferometry; Bragg-edge imaging; neutron

* Corresponding author. Tel.: +1301 975 6465.

E-mail address: daniel.hussey@nist.gov

1. Introduction

At the U.S. National Institute of Standards and Technology (NIST), a new cold neutron imaging instrument will be installed in the spring of 2015 on the cold neutron guide NG-6 and begin operation in summer of 2015. The development of the instrument is expected to proceed over several years, culminating in the world's first neutron microscope. In this article we discuss the initial development phase of the instrument.

2. Description

2.1 Location

The neutron physics group operates the cold neutron guide NG-6 located in the old guide hall of the NIST Center for Neutron Research (NCNR), Nico et al. (2005). The beamline has traditionally served experiments in nuclear physics that study the decay and other fundamental properties of the neutron. Recently, the group began operating a second cold neutron guide which has a factor 4 higher neutron fluence rate, which will improve the statistics of these measurements, and resulted in a vacant end-station at NG-6 which will be the location of the cold neutron imaging instrument (CNII). The NG-6 guide is a straight, ^{58}Ni coated guide, 68 m in length, with cross-section 6 cm wide by 15 cm tall that views the NCNR cold source, which is currently a liquid hydrogen moderator maintained at 20 K. The spectrum is approximately described by a Maxwell-Boltzmann distribution with a characteristic temperature of 40 K and peak wavelength of 0.5 nm. In addition to the end-station, there are three monochromatic beam lines, one of which is located in a guide cut about 20 m upstream of the end of the guide. All three monochromatic beam lines use the bottom half of the guide, leaving the upper half of the guide unobstructed for the end-station. The center of the unobstructed beam viewed by the end-station is about 1.28 m above the floor.

There are several constraints on the first phase of the design. The 30 m small angle neutron scattering instrument located on NG-7 permits a maximum of about 1.25 m space from the beamline center to the east. Maintaining the ability to extract a 0.89 nm beam from the monochromator on beam NG-U permits a maximum of about 2.15 m from the beam line center to the west. This space is sufficient for users to bring ancillary equipment to conduct in situ studies of many samples. To minimize disruptions to the monochromatic beamlines, the existing 6 cm diameter collimator, located about 1 m from the end of the guide and views the unobstructed top half of the guide will remain in place. As well, the location of the end-station shutter will not change in the first phase, so that the maximum flight path will be about 9.5 m. In order to reduce the radiation levels from scattered neutrons and prompt gamma activation, the instrument will be completely enclosed by radiation shields that consist of a welded steel form that is 25 cm wide (labeled 1 in Figure 1) and filled with wax and steel shot, which is the conventional shield design adopted at the NCNR; the layout is shown in Figure 1. The radiation dose rates are shown in Figure 2 for two sample types which completely block the beam, a polyethylene sample to create a strong scattered neutron source and a totally attenuating borated aluminum sample to create a strong prompt gamma source. The radiation calculations are performed with an NCNR developed Monte Carlo n-particle (MCNP) code. The wall shields are nominally 1.2 m wide by 2.3 m tall so that the height of the interior of the enclosure is about 2 m from the floor to the bottom of the roof shields. The roof shields at the upstream and downstream positions have removable sections to permit the installation of cryostats into the beam (labeled 2 in Figure 1). There are two roof sections that have openings for ventilation fans to ensure air flow during experiments that use cryogenics or hydrogen (labeled 3 in Figure 1). One wall shield at the upstream position includes a feed-through to pass hoses and cables for use during neutron microscope imaging experiments. Every other wall shield has a 23 cm \times 23 cm opening at the bottom to permit cables to be passed into the enclosure on an ad hoc basis. There is a floor trench that also enables introducing cables and hoses into the enclosure on a more permanent basis. Access to the enclosure is through a dog-leg that is barricaded by an open wire gate (labeled 4 in Figure 1). This approach was chosen over a massive sliding door to facilitate ventilation of the enclosure and ease of use by experimenters.

2.2 Flight Path

The instrument will feature an optical rail (labeled 5 in Figure 1) that is permanently mounted to the guide hall floor. To ensure the rail is level, a continuous epoxy floor will be poured along the entire length of the instrument with a width of about 63 cm to a thickness of about 1.6 cm (labeled 6 in Figure 1). Once the epoxy resin has hardened, an aluminum plate, 2.54 cm in thickness, will be mounted to the floor on top. The instrument rail will be two 2.54 cm diameter (1") Thompson Rails² separated by 50.8 cm (20"). Optical components will mount to the rail using Roundway bearings to provide a kinematic mount for those devices that are not in constant use.

The flight path will be enclosed by an evacuated flight path that is 30 cm in diameter (labeled 7 in Figure 1). To enable polarized neutron imaging measurements, the flight tubes will be wrapped with wire to create a 5 G solenoidal magnetic field, longitudinal to the beam optic axis. The flight path will be demountable and the length of the flight path can be adjusted in increments of about 76 cm. As well, the flight path can be raised by 15 cm to provide an evacuated flight path for imaging with a double monochromator assembly (mounted near position 8 in Figure 1). An aperture selector (mounted near position 8 in Figure 1) with three positions will be installed on the interior of the cave so that appropriate or custom apertures can be selected and installed for a given experiment. The minimum L/D will be 185 with an estimated fluence rate of $2 \times 10^8 \text{ cm}^{-2} \text{ s}^{-1}$, with a beam size of about 8 cm \times 8 cm; apertures can be made to achieve higher L/D for high resolution imaging at the expense of beam size and neutron fluence rate.

2.3 Conventional Radiography and Tomography

The instrument will provide researchers with conventional neutron radiography and tomography capabilities making use of all detectors (mounted at position 9 in Figure 1) that have been developed and available at the NIST Neutron Imaging Facility at BT2. The currently available scintillators include LiF:ZnS scintillators with resolution of 0.15 mm and 0.3 mm for high frame rate imaging, GadOx scintillators with nominal thicknesses of 7 μm and 20 μm . The scintillators are currently coupled to an Andor Neo scientific complementary metal–oxide–semiconductor (sCMOS) camera using various lenses including Nikon 50 mm f/1.2, Nikon 85 mm f/1.8, Nikon 200 mm f/4, and Nikon 102 mm f/2.4 lenses. Reproduction ratios of each lens can be optimized by use of extension tubes. Soon, an image intensifier will be incorporated into the detector system to improve the low light imaging characteristic of GadOx. The highest frame rate time series that can be obtained with the Neo is 50 Hz; there are plans to purchase a higher frame rate detector for the NIST neutron imaging program in the near future. A large area, high resolution charged-coupled device (CCD) with a 100 megapixel array and 9.5 μm pixel pitch will also be available. In addition to the scintillator-based detectors, researchers can employ the two microchannel plate cross-strip detectors which have active areas (spatial resolutions) of 40 mm diameter (13 μm) and 9 cm \times 9 cm (20 μm). Samples are rigidly mounted to an optical bread board that has tapped holes for 1/4-20 threads on a 2.54 cm [1 inch] spacing that is on top of a 5-axis motorized table (x, y, pitch, roll, and yaw); vertical translation can also be included for experiments that require this axis to be motorized. The horizontal translation is ± 15 cm, the pitch and yaw ranges are $\pm 10^\circ$, and the yaw can rotate continuously. The sample table (labeled 10 in Figure 1) mounts to the instrument rail so that it can be positioned either at the conventional radiography position or at the upstream position for use with in the microscope imaging mode. The neutron beam is limited to the region of interest by an automated beam mask (labeled 11 in Figure 1) composed of lithiated plastic (1 mm in thickness), borated aluminum (1 mm in thickness) and cadmium (1 mm in thickness). At a minimum, the beam is limited to the field of view of the detector system to avoid systematic measurement errors due to the detector system point spread function, Hussey et al. (2013).

² Certain trade names and company products are mentioned in the text or identified in an illustration in order to adequately specify the experimental procedure and equipment used. In no case does such identification imply recommendation or endorsement by the National Institute of Standards and Technology, nor does it imply that the products are necessarily the best available for the purpose.

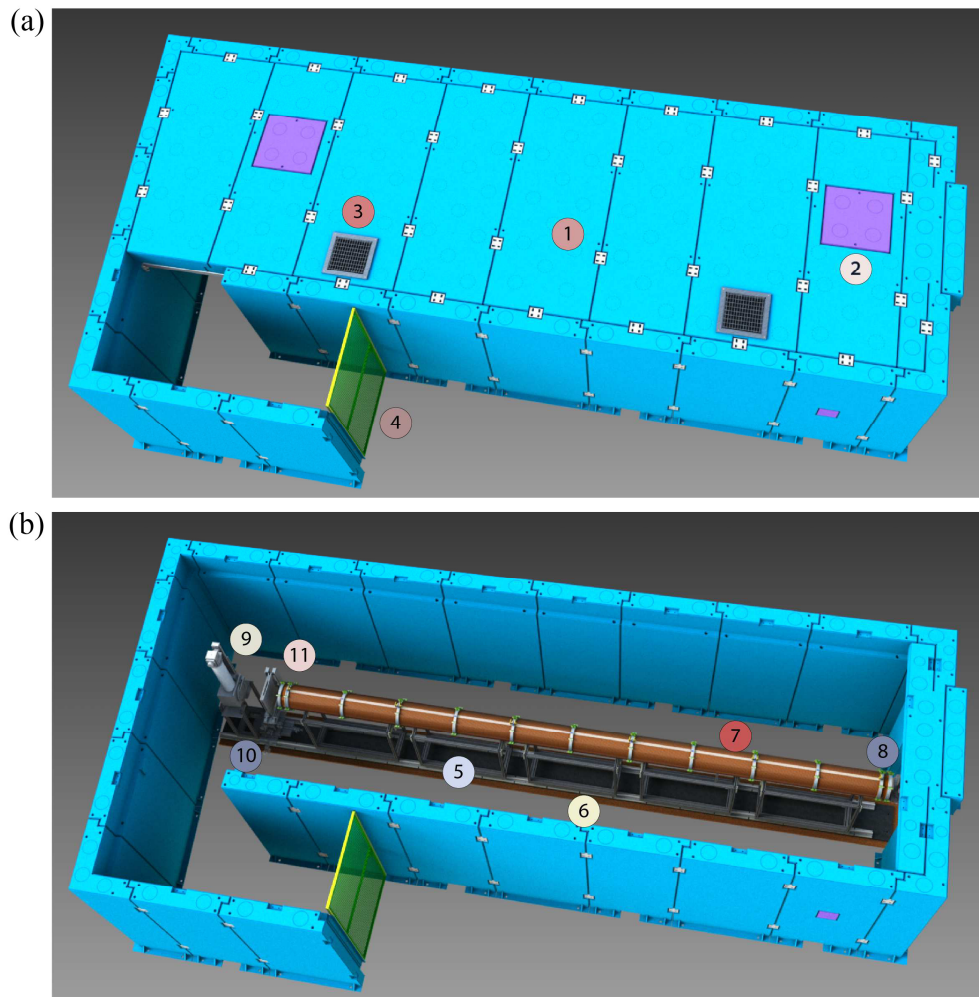


Fig. 1 Sketch of the CNII layout showing the (a) roof shields and (b) the interior space for conventional imaging, east is on the top of the figures, west is on the bottom, see text for identification of labels.

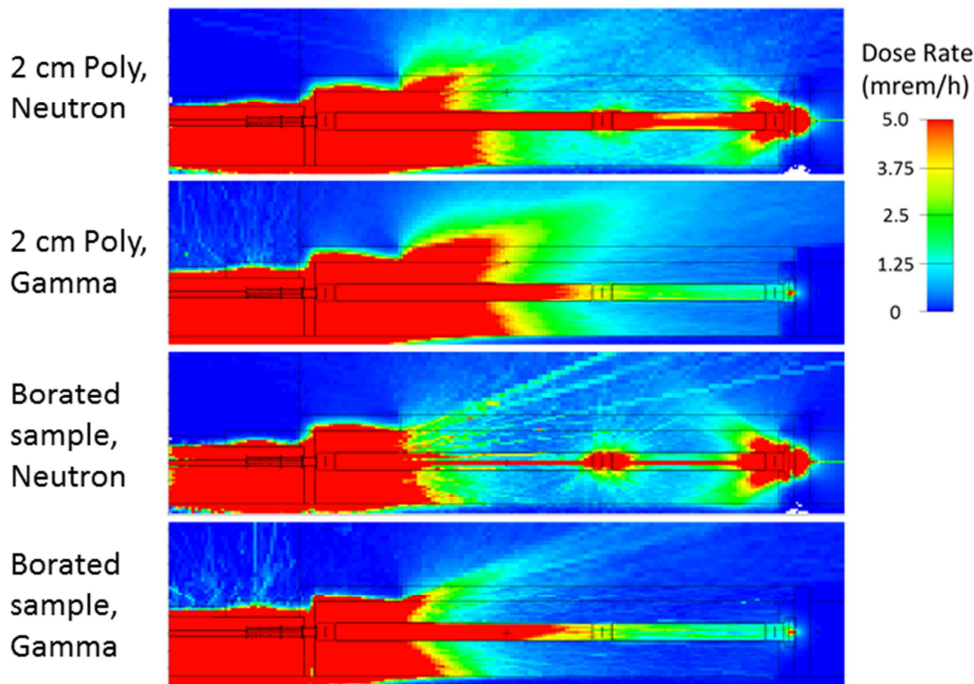


Fig. 2 Dose rates for worst case samples along the center of the beam, the beam comes from left to right, 1 mrem/h is equivalent to 10 μ Sv/h.

2.4 Energy Selective Imaging

An important feature of the instrument is the double monochromator assembly which will be composed of either highly oriented pyrolytic graphite (HOPG) using the (002) reflection or pressed silicon using the (111) reflection. The advantage of the HOPG (002) is the high neutron reflectivity while the advantage of the Si (111) is the elimination of the second order contamination for improved wavelength resolution and the availability of monolithic crystals that can completely capture the beam. Given the spectrum of the end-station, the double monochromator will provide wavelengths in the range of 0.3 nm to 0.6 nm, which will span the largest Bragg-edge of most compounds. The crystals will be separated vertically by 15 cm so that the optical axis of the instrument is translated upwards by 15 cm compared to the use during white beam imaging. The double monochromator assembly will enable energy selective applications including Bragg-edge imaging, Talbot-Lau interferometry and polarized neutron imaging.

In Bragg-edge imaging, one measures the change in the coherent scattering cross section as the wavelength is scanned such that a given crystallographic plane can no longer diffract the neutron. Since the coherent scattering cross section goes as $\lambda^2 F_{\text{HKL}}^2 d_{\text{HKL}}$, the change in cross-section is largest when H, K, L correspond to 1 or 0, where the structure factor, F_{HKL} , and lattice spacing d_{HKL} are both maximum, Vogel et al. (2002). Anticipated applications of Bragg-edge imaging include strain measurements in hybrid welds and determination of chemical composition in electrochemical systems. It is expected that Bragg-edge imaging will be the most used energy selective imaging modality.

In Talbot-Lau neutron interferometry, one is able to measure the neutron phase gradient of a sample in one dimension by measuring the change in position of the Talbot self-image of a phase grating, Pfeiffer et al (2006). The required lateral coherence of the beam is created by using an absorbing grating just downstream of the double monochromator; this source grating has a nominal pitch of 1 mm with a duty cycle of about 40 % and can be

fabricated using laser drilling or electric discharge machining. The phase grating is composed of high aspect ratio ($\sim 10:1$) lines etched in silicon on an $8\text{ }\mu\text{m}$ line spacing. The height of the lines is determined by the neutron wavelength employed so as to modulate the phase of the transmitted beam by π . One can make use of the Talbot self-image that occurs at a fractional distance to the Talbot length so that the geometric unsharpness of the image is reduced. Since the pitch of the Talbot self-image at the $1/8$ th Talbot distance for an $8\text{ }\mu\text{m}$ phase grating is $4\text{ }\mu\text{m}$, one measures the shift of the image position by beating an absorbing grating of Gd which is composed of lines of Gd deposited on a silicon wafer on a $4\text{ }\mu\text{m}$ period, with $2\text{ }\mu\text{m}$ wide openings and about $3\text{ }\mu\text{m}$ Gd thickness. The field of view of both the phase and absorbing gratings is $7\text{ cm} \times 7\text{ cm}$, Lee et al (2009). The absorbing grating will be translated across the beam by use of a piezoelectric actuator which has resolution of 25 nm and $100\text{ }\mu\text{m}$ travel. The phase grating is mounted on a motorized 4-axis alignment system with control over pitch, roll, yaw and longitudinal translation.

Since neutrons possess a magnetic moment and are neutral, they make ideal probes of magnetic material and magnetic fields. A polarized neutron beam will be produced by a continuously polarized ^3He cell making use of spin exchange optical pumping (SEOP). In SEOP, one polarizes a Rb vapor using 795 nm polarized laser light; the polarized $5s$ electron of the Rb atom polarizes the ^3He nucleus via the hyperfine interaction during collisions and the ^3He polarization asymptotically reaches equilibrium with a typical time constant of about 8 h , Chen et al (2011). If the ^3He is not continuously polarized, the polarization decays exponentially, with a typical time constant of order several hundred hours. By developing a ^3He polarization system that is continuously polarized while mounted on the imaging beam, the ^3He polarization (and thus the neutron beam polarization) will remain constant. An additional benefit is that ^3He cells can be made with flat windows so that there is minimal distortion of the flat field, which is not possible using a supermirror polarizer. The system will be mounted just downstream of the double monochromator assembly, with the guide field being supplied by the solenoidal field supplied by the flight path. A similar system is being developed for use with spin analysis after the sample.

2.5 Microscope Imaging

The instrument rail and large enclosed space will enable the instrument to be used for investigating novel imaging and scattering methods. Currently, the method with the most promise is the creation of a neutron microscope using reflective neutron lenses based on Wolter optics, Liu et al (2013). Wolter optics are achromatic and can be designed to exactly cancel coma and spherical aberrations that produce images with good off-axis properties. With a lens, one does not require collimation to obtain high resolution, as is the case with pinhole optics; without the need for collimation the intensity can increase by a factor of over 50 for imaging at a resolution of $15\text{ }\mu\text{m}$. One can create a magnifying lens in which the neutron intensity is magnified at the detector, so that the effective spatial resolution is improved over that achievable by the detector; with a magnification of 10 it will be possible to obtain neutron images with a spatial resolution of order $1\text{ }\mu\text{m}$; using either the 100 megapixel CCD or the 9 cm microchannel plate detector, the field of view will still be about 1 cm . Another advantage is that, with a lens there is a large gap between elements along the beam line, so that one can obtain high resolution images if the sample is in a bulky sample environment such as a pressure vessel. Additionally, for polarized neutron imaging, one could place a spin analyzer downstream of the sample and not lose spatial resolution. Two optics are envisioned for the facility, a $1:1$ optic that will enable high frame rate imaging at a spatial resolution of $15\text{ }\mu\text{m}$ with a time resolution 50-100 times that achievable at the BT2 imaging facility and a $10\times$ magnifying optic to reach $\sim 1\text{ }\mu\text{m}$ spatial resolution. The $1:1$ optic is expected to be available for users in 2017 and the $10\times$ optic is expected in 2018.

3. Conclusions

The new cold neutron imaging instrument at NIST will support a broad range of neutron imaging modalities, including conventional neutron radiography and tomography, energy selective techniques, and the novel neutron microscope. Given the instrument layout, researchers will be able to incorporate other neutron optical components

or sample environments. When fully developed, the Wolter optics will enable the instrument to achieve unprecedented time and spatial resolution in neutron imaging.

Acknowledgements

This work was supported by the U.S. Department of Commerce, the NIST Radiation and Physics Division, the Director's office of NIST, the NIST Center for Neutron Research, and the Department of Energy interagency agreement No. DE_AI01-01EE50660.

References

- W C Chen, T R Gentile, C B Fu, S Watson, G L Jones, J W McIver, D R Rich, 2011, Polarized ^3He cell development and application at NIST, *Journal of Physics: Conference Series* 294, 012003.
- D.S. Hussey, K.J. Coakley, E. Baltic, D.L. Jacobson, 2013, Improving Quantitative Neutron Radiography Through Image Restoration, *Nuclear Instruments and Methods in Physics Research A* 729 316–321.
- D. Liu, D. Hussey, M. V. Gubarev, B. D. Ramsey, D. Jacobson, M. Arif, D. E. Moncton, and B. Khaykovich, 2013, Demonstration of Achromatic Cold-Neutron Microscope Utilizing Axisymmetric Focusing Mirrors, *Applied Physics Letters* 102, 183508.
- J. S. Nico, M. Arif, M. S. Dewey, T. R. Gentile, and D. M. Gilliam, 2005, The Fundamental Neutron Physics Facilities at NIST, *Journal of Research of the National Institute of Standards and Technology* 110, 137-144.
- F. Pfeiffer, C. Gruenzweig, O. Bunk, G. Frei, E. Lehmann, and C. David, 2006, Neutron Phase Imaging and Tomography, *Physical Review Letters* 96, 215505.
- Seung Wook Lee, Daniel S. Hussey, David L. Jacobson, Cheul Muu Sim, Muhammad Arif, 2009, Development of the Grating Phase Neutron Interferometer at a Monochromatic Beam Line, *Nuclear Instruments and Methods in Physics Research A* 605, 16–20.
- S. Vogel, M.A.M. Bourke, J.C. Hanan, H.-G. Priesmeyer, E. Uestuendag, 2002, Non-Destructive In-Situ Real-Time Measurements of Structural Phase Transitions Using Neutron Transmission, *Advances in X-ray Analysis* 44, 75-84.